In: Mountain Ecosystems ISBN 978-1-61209-306-2
Editor: Kevin E. Richards, pp. 101-121

Chapter 5

ATMOSPHERIC CARBON DIOXIDE TRANSPORT OVER MOUNTAINOUS TERRAIN

Jielun Sun*
National Center for Atmospheric Research, Boulder, Colorado, USA
Stephan F.J. De Wekker
University of Virginia, Charlottesville, Virginia, USA

Abstract

We investigated trace gas transport by daytime mountain-induced circulations based on aircraft data collected during the Airborne Carbon in the Mountains Experiment (ACME04) conducted in 2004. Using measurements of traditional meteorology and trace gases associated with ecosystem processes, we found evidence of thermally-induced vertical mountain circulations consisting of an upslope flow, a horizontal return flow, and a descending flow along the Front Range of Colorado. Turbulent air was generated by convective buoyancy along the mountain slopes and ridges and by strong shear at the mountain ridge tops. The deep turbulent mixed layer was subsequently advected by the ambient large-scale and return flows across the plains east of the Front Range. The descending flow over the plains increased the atmospheric stability, which reduced the vertical mixing above the convective boundary layer over the plains. The mountain circulation and its interaction with the ambient flow and convective turbulent mixing effectively transported the air with its unique

*E-mail address: jsun@ucar.edu (Corresponding author)

characteristics of the CO_2, water vapor, and CO concentrations at the bottom of the atmosphere over the plains to above the convective boundary layer over the plains. This study suggest that mountain-induced circulations can have significant impacts on estimates of the regional ecosystem-atmosphere carbon exchange.

Keywords: atmospheric boundary layer, carbon dioxide, complex terrain, mountain circulation

1. Introduction

Significant progress has been made in investigating mesoscale circulations in complex terrain and their importance in weather forecasting, cloud formation, aviation, and air pollution transport (e.g., Geiger et al., 1995; Whiteman, 2000; Rotach and Zardi, 2007). However, turbulence characteristics of mountain-induced circulations and the role of the mountain-induced circulation in transporting biogenic and anthropogenic trace gases have not been fully investigated. The effect of mountains on the atmosphere is especially important around the Colorado Rocky Mountains, which is evident from the frequent occurrence of turbulent events encountered by commercial aircraft (Wolff and Sherman, 2008).

Air flows can be influenced by two types of mountain forcing. The mechanical forcing of the air flow over and around mountains has been studied in field experiments, in wind tunnels, and with numerical models (e.g., Blumen, 1990). The air flow over mountain tops can be compressed and the air speed enhanced, which leads to turbulence generation. Air flows over mountainous terrain can also be influenced by daytime solar heating and nighttime longwave radiative cooling of mountains (Whiteman, 2000). Because of the solar heating of mountains during the day, the air temperature over the mountain is warmer than the air at the same altitude above the plains that surround the mountain. The difference between the vertically-integrated temperature over the mountain and the plains leads to a horizontal gradient of the atmospheric pressure, which drives the air towards the mountain and leads to an upslope flow. The forcing of the air flow is related to the thermal difference of the mountain and the air at the same altitude, and is referred to as thermal forcing, in contrast to the mechanical forcing mentioned earlier. At night, the radiative cooling of the mountain reverses the thermal forcing and leads to a downslope flow. Both mechanical

and thermal forcing can influence the air flow over the mountain, and the latter has a distinctive diurnal cycle.

The nighttime downslope flow has been studied in great detail. For example, the influence of the ambient large-scale flow on the nocturnal downslope flow was studied during the Atmospheric Studies in Complex Terrain (ASCOT) in the early 1980s (Barr and Orgill, 1989). The nighttime downslope flow occurs not only over steep valleys (Orgill et al., 1992) but also over seemingly flat terrain (Mahrt and Larsen, 1990). The downslope flow transports cold air downward, leading to stably stratified cold air pools and suppressed turbulent mixing over the plains. Recently, the important role of the nighttime downslope flow in transporting ecosystem respired CO_2 and ground-evaporated moisture has been investigated (e.g., Sun et al., 2007; Kutsch et al., 2008; Aubinet, 2008; Sun et al., 2010). As a result of the nighttime downslope flow and cold-air pooling, the air over the plains is characterized by cold, moist, and CO_2-rich air as well as by pollutants, such as CO and aerosols, if the plains are urbanized.

As the thermal forcing of complex terrain reverses after sunrise, the upslope flow induces a vertical mountain circulation. For a two-dimensional mountain with a long mountain ridge and a weak ambient flow perpendicular to the mountain ridge, the thermally-forced mountain circulation (hereafter, mountain circulation) is mainly in the vertical plane. Bounded by mass conservation, the daytime mountain circulation theoretically consists of an upslope flow, a return flow, which is the upslope flow turning away from the mountain, and a descending flow over the plains (e.g., Geiger et al., 1995). If the ambient wind is strong, it can flow over the mountain ridge to the lee side of the mountain. In this situation, the mountain circulation can be confined below the mountain ridge top or completely embedded in the dominant ambient wind. In reality, interactions among the large-scale ambient flow, the upslope flow, and the convective boundary layer over the plains make the observation of the return flow difficult (e.g., McGowan, 2004; Reuten et al., 2005).

The development of the upslope flow depends on several factors, such as the orientation of the slope, the incident solar radiation, and the strength of the ambient wind. The upslope flow has been found to begin one to two hours after sunrise (Orgill, 1989; Whiteman, 1989). Because of the stronger stratification in the cold air pool over the plains compared to that over the slope, the morning development of the convective boundary layer (CBL) over the slope and the mountain ridge is faster than the development over the plains (e.g., Banta, 1984; 1986; Rotach et al., 2004). Therefore, cold air, trace gases, and pollutants at

the bottom of the atmosphere over the plains can be transported upward by both the upslope flow and the vertical convective turbulent transport (e.g., Gudiksen and Shearer, 1989; Kalthoff et al., 2000). The upslope flow leads to an efficient upward transport of moisture, pollutants and aerosols (e.g., Banta, 1984; McKendry et al., 1998; De Wekker et al., 2004). Interactions among the mountain circulation, the ambient flow, and the turbulent mixing can also lead to a deep turbulent mixed layer above the mountain ridge. When advected downwind from the mountain by the ambient and return flows, this layer frequently transitions to an elevated mixed layer over the plains (e.g., Arritt et al., 1992). The vertical coupling between the elevated turbulent layer and the CBL over the plains can lead to a rapid breakup of the cold air pool (e.g., Banta, 1984; 1985; 1986; Whiteman, 1982a & b). On the other hand, the descending flow of the mountain circulation can lead to enhanced stratification above the plains (e.g., De Wekker, 2008). In contrast to the nighttime downslope flow in transporting the ecosystem-respired CO_2, the daytime mountain circulation can transport the nighttime-accumulated CO_2-rich air upslope (Sun et al., 2010).

Direct observations of interactions between mountain circulations and convective turbulence over sunny slopes as well as the vertical transport of CO_2 by mountain circulations, especially airborne observations, have been sparse. Recent examples include two CARBOEUROPE airborne field campaigns, one in Southwestern France (Dolman et al., 2006; Ahmadov et al., 2007) and one in Spain (Pérez-Landa et al., 2007a & b), which were conducted to estimate the regional carbon balance. In this study, we focus on aircraft observations over the Front Range of the Colorado Rocky mountains to investigate the role of the daytime mountain circulation in transporting trace gases, such as CO_2, CO, and aerosols. Our unique aircraft observations include a large number of soundings, turbulence measurements, and a suite of trace gas measurements. The trace gas measurements allow a systematic investigation of 1) dynamic aspects of mountain circulations by using trace gasses as tracers, and 2) trace gas transport by mountain circulations and turbulent mixing under a variety of ambient wind and stability conditions. We summarize the dataset used in the study in section 2. In section 3, we focus on characteristics of the daytime mountain circulation and use trace gases, such as CO_2, to identify the mountain circulation. In addition, we investigate the spatial and diurnal variation of the CO_2 concentration as a result of the mountain circulation. A summary and the implication of the observed transport of CO_2 by the mountain circulation on the regional CO_2 budget are given in section 4.

2. Observations

The data used in this study were collected during the Airborne Carbon in the Mountains Experiment (ACME04) in 2004 (Sun et al., 2010). A total of 16 flights were conducted with the C-130 aircraft from the National Center for Atmospheric Research (NCAR). In general, four flight patterns were flown during ACME04: 1) the racetrack, 2) the roller coaster, 3) the slant and spiral sounding, and 4) the Hayman fire. In this study, we concentrate on the flight patterns of the roller coaster and the spiral runs over the Front Range of the Colorado Rocky Mountains (Fig. 1). The roller coaster run consisted of a terrain following flight across the eastern slope of the Front Range (blue track in Fig. 1), which was commonly combined with the spiral sounding run (orange track in Fig. 1) located $\sim$ 35 km east of the Front Range mountain ridges. Sometimes, a level run at $\sim$ 5000 m altitude was added to connect the roller coaster and the spiral runs.

Wind, temperature, and water vapor were measured by fast response sensors on the aircraft and sampled at 25 samples per second, the CO_2 and CO concentrations at five samples per second, and O_3 and aerosol concentrations at one sample per second. The variability of the data from the fast-response sensors can be used to identify turbulent air. The zero value of the vertical velocity is within the calibration uncertainty; therefore, its fluctuation, not its mean value, was used in the study. Potential temperature, which is conserved as an air parcel moves vertically without any energy exchange with its environment, was calculated from the observed air temperature (e.g., see Wallace and Hobbs, 2006). Water vapor specific humidity, which is the mass of the water vapor for a given mass of air, was used to describe the moisture content of the atmosphere. To ensure the accuracy of the CO_2 concentration measurements, an on-board calibration procedure was carried out frequently during each flight, resulting in data gaps. During ACME04, a ground-based field campaign named the Carbon in the Mountains Experiment (CME04) was conducted at the Niwot Ridge Long-Term Ecological Reserve (LTER) site, which is also an AmeriFlux site in Colorado. The site is located directly under the roller coaster track (marked as the triangle in Fig. 1). All the aircraft and ground measurements and their accuracies were described by Sun et al. (2010).

We analyzed two flight days in this study: the morning research flight 11 (RF11) on 22 July, and the morning and afternoon research flights, RF12, and RF13, on 26 July. The weather conditions during those flights were mostly clear to partly cloudy with relatively weak ambient westerlies (Fig. 2). A significant

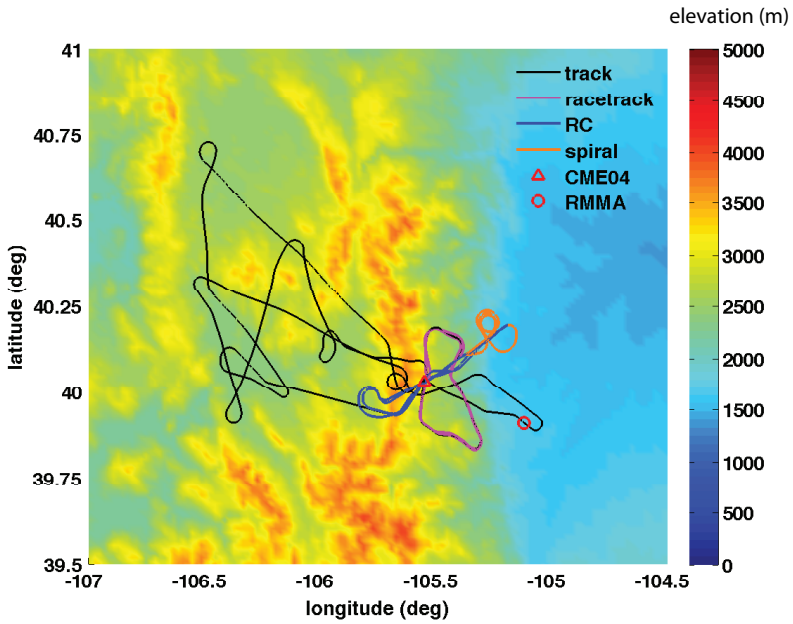

Figure 1. Flight track of RF12, which shows the racetrack, the roller coaster and the spiral tracks, and the location of CME04. The NCAR C-130 aircraft operated from the Rocky Mountain Metropolitan Airport (RMMA) during ACME04.

two-day rain event occurred after RF11. The sunny weather, which occurred the day before RF12, led to large downward CO_2 fluxes. We use local standard time (LST), which is seven hours behind Coordinated Universal Time (UTC). The vertical coordinate used in this study is the pressure altitude above sea level (ASL).

3. Characteristics of Daytime Mountain Circulations and Their Transport of CO_2

The flights over the Front Range allow an investigation of the dynamics of the daytime mountain circulation and trace gas transport by the mountain circulation. We first focus on RF11 to investigate the morning mountain circulation. Then we examine the temporal variation of the mountain circulation by ana-

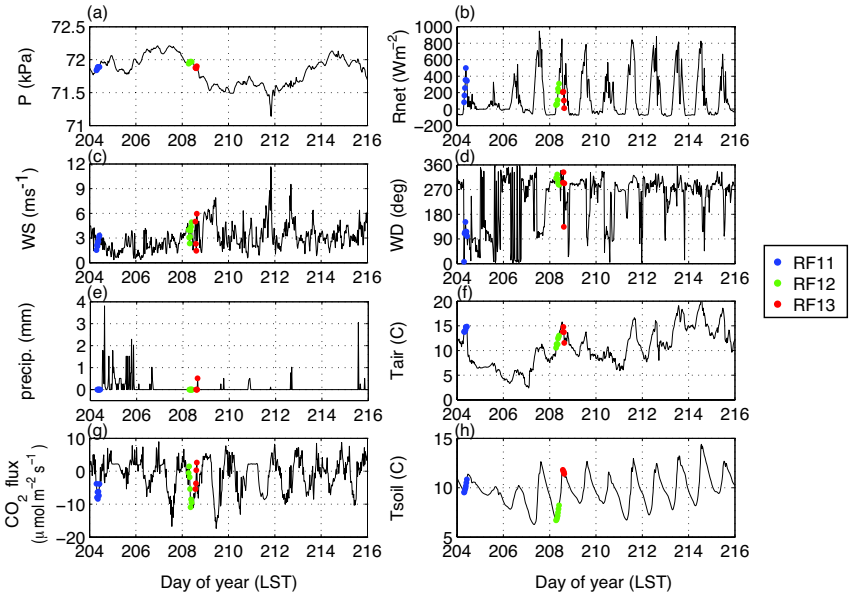

Figure 2. The time series of (a) air pressure (P) at 12 m above the ground, (b) net radiation (Rnet) at 25 m, (c) wind speed (WS), and (d) direction (WD) at 21 m, (e) precipitation at 10.5 m, (f) air temperature (Tair), (g) CO_2 flux at 21 m, and (h) soil temperature (Tsoil) at 5 cm depth at one of the CME04 towers operated by the University of Colorado. The three flights that were analyzed in this study are marked with three different colors on each time series.

lyzing the observations from RF12 and RF13 that were conducted on the same day.

3.1. 22 July

In the early morning of RF11, the aircraft descended along the sunny slope following the roller coaster track, spiraled up to about 5000 m, and flew southwestward along the roller coaster track at 5000 m (Figs. 3a and b). The air over the plains was relatively stable, which was evident in the increasing potential temperature with height (Fig. 3f), and the decreasing water vapor and CO_2 concentrations with height (Figs. 3g and h). The mountain ridge height along the Front Range is around 3600 m. It peaks at $\sim$ 3450 m along the roller coaster

track (marked z_{top} in Fig.3), and $\sim$ 3900 m west of the spiral run. The relatively high water vapor and CO_2 concentrations at the bottom of the atmosphere over the plains are due to the combined effect of the ground evaporation and ecosystem respiration during the previous night and the weak vertical turbulent transport as a result of the stably stratified nocturnal atmosphere boundary layer. Ground heating after sunrise at 0449 LST produced convective turbulent mixing along the sunny slope as evident from CME04 (Sun et al., 2010; Burns et al., 2011). The relatively low turbulence strength as demonstrated in weak fluctuations of the vertical velocity far below the mountain ridge (Fig.3e) indicates that the CBL along the sunny slope was below the aircraft flight level at the time. The upper air over the plains was less turbulent than the air over the sunny slope at the same altitude.

The daytime thermally-forced upslope flow, opposite from the ambient westerlies, was evident from the easterly wind below $\sim$ 2900 m along the roller coaster run (marked z^b_{EML} in Fig. 3) and below $\sim$ 3100 m from the spiral run (Fig. 3d). The difference in the depth of the easterly flow at the two locations probably results from the spatial variation of the combined large-scale pressure forcing and the thermal forcing associated with the variation of the Front Range mountain ridge heights. As the upslope flow encountered the ambient air flowing down the mountain ridge along the sunny slope at z^b_{EML} in Fig. 3, the convergence led to the eastward transport of the convective turbulence that had developed along the sunny slope. Because the eastward return flow was in the same direction as the ambient wind in this case, the return flow appeared as an enhancement of the wind speed just above z^b_{EML} (Fig. 3c). In addition, the enhancement of the water vapor and CO concentrations from the upslope transport of the plains air was also observed in Figs. 3g and i. Because of the existence of the urban area at the Front Range, the observed high CO concentration (Fig. 3i) was likely associated with anthropogenic pollution (Seinfeld and Pandis, 2006). The simultaneous increase of the water vapor, the CO concentration, and the wind speed above z^b_{EML} confirmed the presence of the return flow as part of the thermally-forced vertical circulation, which is schematically shown in Fig. 4. If the return flow carried part of the plains air, we would expect the CO_2 concentration to increase above z^b_{EML}, which was not clearly evident in Fig. 3h. The absence of the clear CO_2 enhancement is partly due to the missing CO_2 observation below z^b_{EML} because of the CO_2 sensor calibration. In addition, as the boundary layer air over the plains was transported upward by the upslope flow along the sunny slope, the high CO_2 concentration could be reduced by

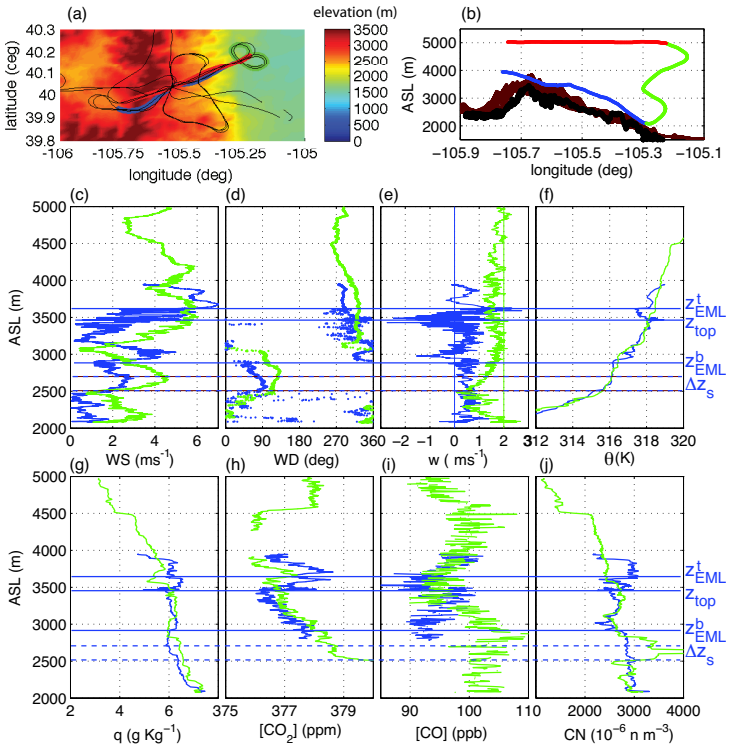

Figure 3. The aircraft observations along the roller coaster run (blue), and the spiral run (green) during RF11. The two runs were flown consecutively at 0622 LST and 0627 LST. Their flight tracks and the topography are in (a). Their altitudes are in (b), where the topography under the roller coaster run is in black, and the topography west of the spiral run is in brown. The observations include (c) wind speed, (d) wind direction, (e) vertical velocity, (f) potential temperature, (g) water vapor specific humidity, and the concentrations of (h) CO_2, (i) CO, and (j) aerosols as functions of altitude. For easy comparison, the vertical velocity for the spiral run is shifted by 2 ms^{-1}, and the zero vertical velocity for each run is marked in its track color in (e). The approximate bottom and top of the elevated mixed layer (EML) for the roller coaster run are marked with the horizontal lines and labeled z^b_{EML} and z^t_{EML}, respectively. The mountain top under the roller coaster run is marked z_{top}. The relatively stable layer, Δz_s, as a result of the descending flow of the mountain circulation, is marked with the dashed lines.

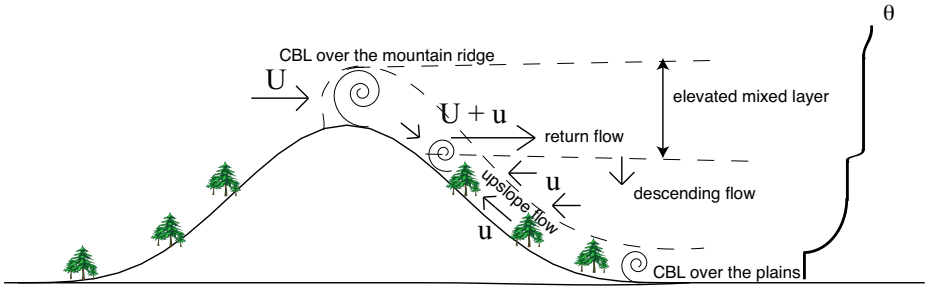

Figure 4. Schematic summary of the morning mountain circulation and the simplified potential temperature (θ) profile over the plains downstream from the mountain from RF11. Here, U and u represent the ambient westerly flow, and the thermally driven upslope flow. The spiral symbols represent turbulent air. The dashed line along the slope represents the top of the convective boundary layer (CBL). The approximately horizontal dashed lines represent the top and the bottom of the elevated mixed layer (EML).

both photosynthetic uptake of mountain vegetation and the upward convective turbulent mixing along the slope, and were observed on the slope surface at CME04 (Sun et al., 2010; Burns et al., 2011). By contrast, water vapor release as a by-product of photosynthesis as well as soil evaporation can enhance the air water vapor content. The upslope transport of the air along the eastern slope of the Front Range was also evident from the carbon isotope analysis by comparing the air samples collected by the aircraft and at the CME04 site (Sun et al., 2010). Because of the uncertainty of the zero velocity calibration, the descending portion of the mountain circulation cannot be directly measured by the aircraft. However, its effect in stabilizing the atmosphere was visible between $\sim$ 2500 m and $\sim$ 2750 m from the roller coaster run (marked by Δz_s between the dashed lines in Fig. 3) in 1) the reduced high-frequency oscillation of the vertical velocity, 2) the increased air temperature, 3) the reduced water vapor, and 4) the increased wind speed as a result of the reduced turbulent mixing.

Near the mountain ridge top (z_{top} in Fig. 3), the strong wind shear associated with the strong westerly ambient flow and buoyant turbulence led to the strongly turbulent CBL in the layer that was slightly below z_{top} and z^t_{EML}

in Fig. 3e. As a result of the turbulent mixing within the CBL, the potential temperature and the water vapor specific humidity were almost invariant with height in this layer (Figs. 3f and g). The higher concentrations of CO_2, water vapor, and aerosols, and the lower CO concentration within the CBL compared to those below the mountain ridge top (Figs. 3g, h, and j) could be natural and anthropogenic. Naturally, the air close to the mountain ridge top could be related to the soil respiration and evaporation above the tree line of $\sim$ 3300 m, and possible CO deposition to soil surfaces at night (e.g. Conrad and Seiler, 1985). Anthropogenically, the efficient power plant at Hayden, Colorado, upstream of the roller coaster run could also lead to the high CO_2, water vapor, and aerosol, and low CO concentrations. Because of the magnitude of the CO_2 and CO change with height, the observed high-CO_2 and low-CO air above z_{top} is more likely associated with the power plant upstream. The sharp reduction of the turbulence above $\sim$ 3600 m (marked z^t_{EML} in Fig. 3) could be due to lack of buoyancy either above the top of the CBL over the mountain ridge top or over the shady west side of the mountain as the aircraft flew across the sunny and shady sides of the mountains below the top of the CBL over the mountain ridge (see Fig. 4 for the schematic). If the latter was true, the depth of the turbulent layer over the sunny side of the mountains would be higher than z^t_{EML}.

Downstream of the Front Range mountains, turbulence was enhanced above the elevation of the convergence zone on the sunny slope, and was further enhanced close to the mountain ridge top. Advected by the ambient and the return flows, the deep turbulent layer was extended downstream from the mountains as an elevated mixed layer (EML) above the relatively stable upper-level air over the plains. The dynamical and ecological processes contributed to the variability in CO_2, CO, water vapor, and aerosol concentrations, and the formation of the sublayers downstream from the mountains. The observed EML from RF11 was turbulent but not well mixed in the vertical, which is similar to the results from the numerical simulations over the Front Range by Arritt et al. (1992).

Due to turbulence energy dissipation, the turbulence intensity decreased with distance from the Front Range mountains. However, the EML was still visible in the vertical velocity oscillation from the spiral run between $\sim z^b_{EML}$ and 4000 m (Fig. 3e). The higher top of the turbulent layer ($\sim$ 4000 m) compared to the top of the turbulent layer from the roller coaster run (z^t_{EML} in Fig. 3) is more likely due to the higher mountain ridge tops upwind of the spiral run compared to those along the roller coaster run (Fig. 3b). The relatively low CO_2 and high CO concentrations above 4000 m observed from the spiral run

may represent the previous daytime air from a few hundred of kms upstream transported by the ambient westerly flow during the previous night. The low CO_2 concentration could result from the combined effect of ecosystem photosynthesis and convective mixing over a deep atmospheric boundary layer. The high CO concentration could be due to anthropogenic emissions, possible biogenic photoproduction (e.g., Tarr et al., 1995), and abiotic processes associated with chemical oxidation of soil organic matter (e.g., Conrad and Seiler, 1985). Figure 4 shows a schematic summary of the important processes during the morning mountain circulation that were derived from the RF11 analyses.

3.2. 26 July

The temporal variation of the mountain circulation from morning to early afternoon was investigated by analyzing two sets of the roller coaster and spiral runs from RF12 and one set from RF13. The three roller coaster runs were flown at $\sim$ 0733, 0839, and 1437 LST (Fig. 5), and the three spiral runs were flown at $\sim$ 0740, 0844, and 1442 LST (Fig. 6).

At the time of the first roller coaster and spiral runs (blue traces in Figs. 5 and 6), a stably-stratified air layer below the convergence zone (blue z^b_{EML} in Fig. 5) was observed in both the potential temperature (Figs. 5f and 6f) and the vertical velocity (Figs. 5e and 6e), which was similar to the air flow during RF11. Compared to RF11, the stronger ambient northwesterly flow resulted in the northwesterly flow along the roller coaster run down to $\sim$ 2450 m (marked with blue z^b_{EML} in Fig. 5), which was about 400-500 m lower than the one from RF11. The ambient flow was observed above $\sim$ 2500 m along the spiral run (marked blue z^b_{EML} in Fig. 6). The flow at the bottom of the atmosphere over the plains was influenced primarily by a high-pressure system southeast of the flight location as well as by thermal forcing of the mountains; therefore, it was southerly, instead of easterly, for the two morning runs. The differences in the CO_2, CO, and water vapor concentrations above and below the altitude where the ambient westerly flow and the southerly flow converged (blue z^b_{EML} in both Figs. 5 and 6) were due to the characteristics of the different air masses. Again, the high CO_2 and aerosol, and low CO air was observed close to the mountain ridge top (between blue z_m and z^t_{EML} in Fig. 5), which indicate the possible effect of the power plant upstream for the roller coaster run as explained in the previous subsection. The high CO_2 and relatively high CO and aerosol air above the blue z^t_{EML} may reflect the previous daytime CBL air upstream.

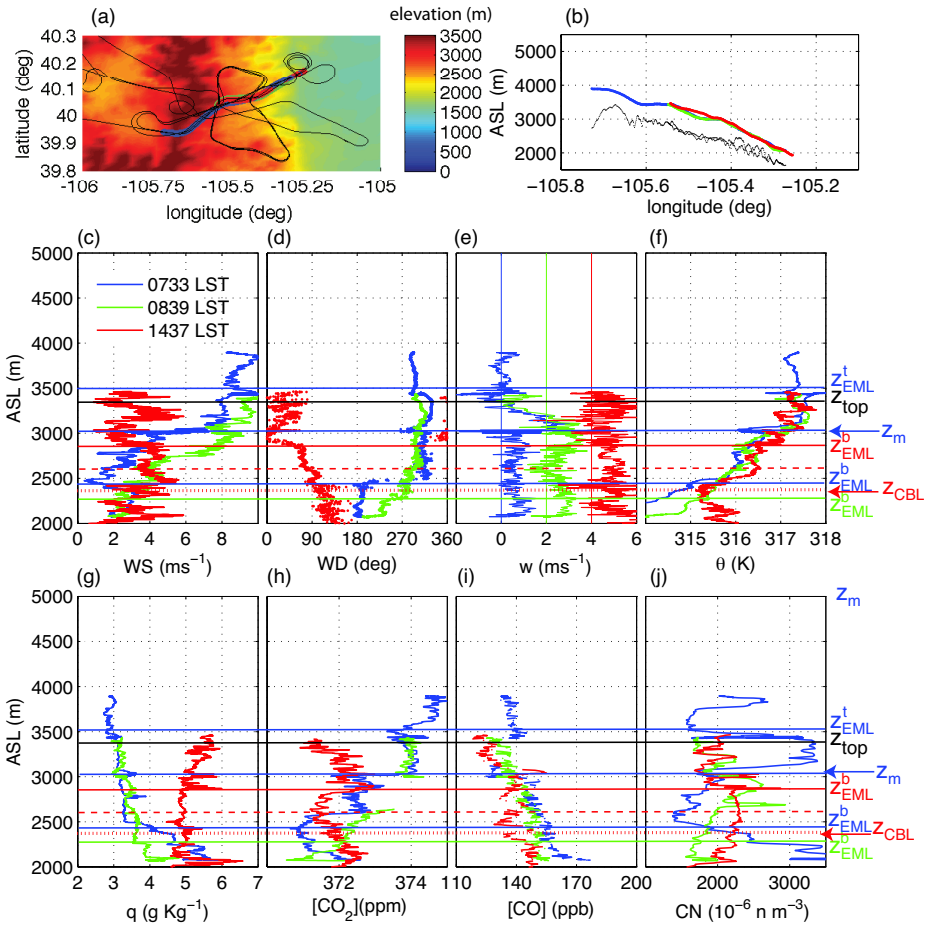

Figure 5. The aircraft observation of (c) wind speed, (d) wind direction, (e) vertical velocity, (f) potential temperature, (g) water vapor specific humidity, and the concentrations of (h) CO_2, (i) CO, and (j) aerosol as functions of altitude along the roller coaster run at 0733 LST (blue) and 0839 LST (green) from RF12, and at 1437 LST (red) from RF13. The flight tracks are marked in (a) and their altitudes are in (b), where the topography is colored in (a) and in black in (b). The top and bottom of the EML for each run are marked with z^t_{EML} and z^b_{EML} in the color of the track, respectively. Because the z^t_{EML} at 0839 LST and 1437 LST were above the flight track, no green and red z^t_{EML} are in this plot. The vertical layer between the red z^b_{EML} and the red dashed line marks the relatively stable layer associated with the descending flow for that run. The red dotted line marks the top of the CBL over the plains at the time of RF13. The black line labeled with z_{top} marks the top of the mountain ridge along the roller coaster track. The blue z_m marks the bottom of the ambient air flow that was not strongly influenced by the eastern slope.

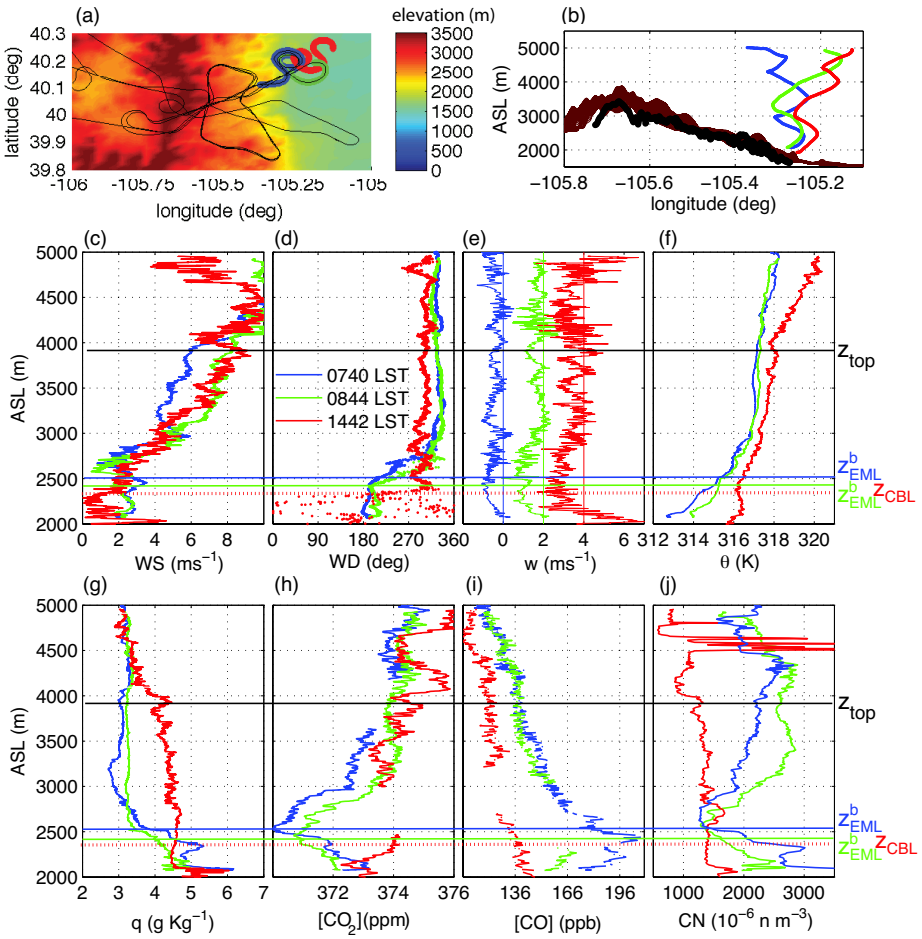

Figure 6. The same as Fig. 5 except for the three spiral runs east of the Front Range. The topography upwind of the spiral run and along the roller coaster run are marked in brown and black in (b), respectively. Here, z_{top} marks the approximate mountain ridge top upwind of the spiral run.

At 0839 LST (green traces in Figs. 5 and 6), the northwesterly ambient wind strengthened. The convergence between the ambient northwesterly and the southerly flows propagated down along the sunny slope (marked green z^b_{EML} in Figs. 5d and 6d). The downslope movement of the ambient northwesterly flow was also visible in 1) the enhanced turbulence, 2) the increased potential temper-

ature, and 3) the increased CO_2 concentrations from the 0839 LST run between the blue and green z^b_{EML} along both roller-coaster and spiral runs (Figs. 5 and 6).

After refueling, the aircraft went back and flew another set of the roller coaster and spiral runs (red traces in Figs. 5 and 6). By then the air had become strongly turbulent up to $\sim$ 2400 m (marked red dotted line with z_{CBL} in both Figs. 5 and 6) over both the eastern slope and the plains. Along the roller coaster run, the evaporation, ecosystem photosynthesis, and the turbulent mixing led to warming, increased water vapor content, and decreased CO_2 concentration over the plains CBL. The flow from the ground up to $\sim$ 2800 m along the eastern slope (marked red z^b_{EML} in Fig. 5) changed from the morning southerly to the easterly upslope direction. In contrast, the wind direction over the plains was about the same as the ambient northwesterly wind all the way down to the top of the CBL (marked with red z_{CBL} in Fig. 6). The absence of the upslope flow at the location of the spiral run indicates that the influence of the thermal forcing of the Front Range on the air flow was limited to the area close to the Front Range. The reduced thermal forcing could be associated with the cloud development as shown in the reduced net radiation and reduced CO_2 fluxes at CME04 during the time of the afternoon flight (red marks in Figs. 2b and g). As a result of the reduced CO_2 uptake by vegetation and the reduced vertical turbulent mixing in response to the reduced downward solar radiation, the CO_2 and CO concentrations decreased with height along the eastern slope. When the ambient and upslope flows converged at $\sim$ 2800 m (red z^b_{EML} in Fig. 5), once again, the upslope flow along the eastern slope transported the air with relatively high CO_2, water vapor, and aerosol concentrations from the bottom of the CBL over the plains to above the convergence altitude. The relatively stable layer, as visible between the red z^b_{EML} and $\sim$ 2600 m (marked with red dashed line in Fig. 5) in the reduced high-frequency oscillation of all the variables, was probably associated with the descending flow as part of the mountain circulation.

Because the mountain circulation was limited to the area close to the Front Range as seen from the absence of the easterly flow, the strong turbulence above 4000 m along the spiral run reflected the upwind atmospheric characteristics northwest of the run, where the air could be influenced by the mountain circulation close to the Front Range. Along the spiral run, both water vapor and CO_2 concentrations were well mixed vertically between the plains CBL top and 4000 m (Figs. 6g and h). Within this layer, the water vapor specific humidity

increased from its morning value of 3 g kg $^{-1}$ to 4.5 g kg $^{-1}$. The CO_2 concentration at 2500 m increased from its morning value of 371 ppm to 374 ppm. The largest CO_2 concentration from the entire RF13 flight path was over the high mountain peaks (Fig. 7). This result indicates that ecosystem respirated and anthropogenic CO_2 were transported above the mountain peaks, and the photosynthetic reduction of the CO_2 had not reduced the relatively high CO_2 concentration at those altitudes by the time of the flight, even with the help of the daytime convective turbulent mixing and the thermally-induced mountain circulation.

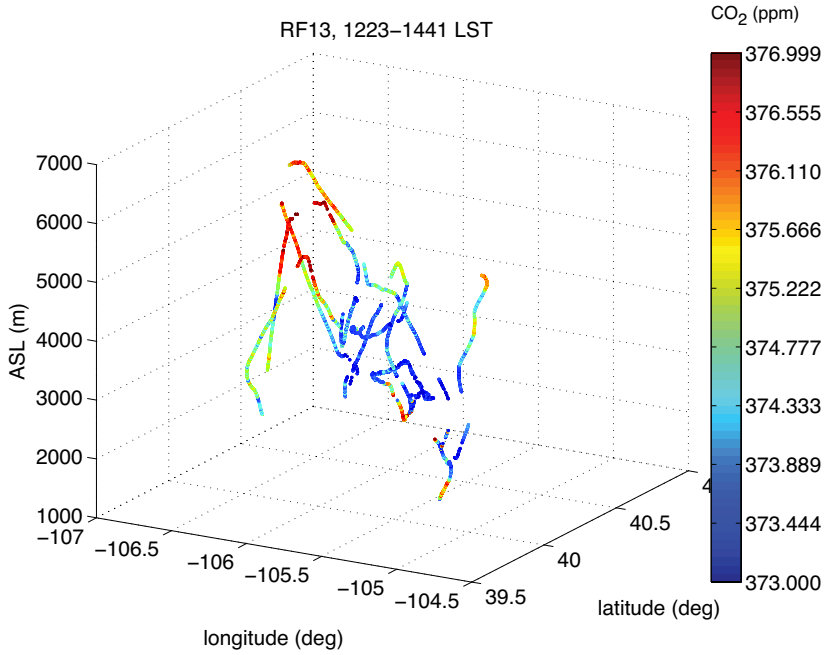

Figure 7. The CO_2 concentrations along the flight path during RF13 .

4. Conclusion

Using unique trace-gas and traditional meteorological observations on board the NCAR C-130 aircraft, we investigated interactions between thermally-induced mountain circulations and convective turbulent mixing and their impact on the

transport of trace gases, such as CO_2, over the Colorado Front Range. Using the consistent observations from both traditional meteorology and known characteristics of the air associated with ecosystem activities at the bottom of the atmosphere over the plains, we identified a vertical mountain circulation over the Colorado Front Range. Because of the north-south oriented mountain ridge of the Front Range, the daytime mountain circulation east of the Front Range was found to be close to a two-dimensional vertical circulation. Bounded by mass conservation, it consisted of the upslope flow along the sunny slope west of the plains, the horizontal return flow away from the mountain and above the altitude where the upslope flow and the downslope ambient flow converge, and the descending flow over the plains. As a result of 1) the convergence between the upslope flow and the opposite ambient flow, 2) the convective mixing over the sunny slope and mountain ridge, and 3) the strong shear generated turbulent mixing close to the mountain ridge top, the air transported up by the upslope flow transitioned to a relatively deep turbulent layer above the convective boundary layer over the plains.

We found that as a result of the daytime mountain circulation, the air at the bottom of the convective boundary layer over the plains could be transported by the upslope flow to the elevated mixed layer above the convective boundary layer over the plains. We observed evidence of the upslope transport of the nighttime-accumulated moist, CO_2 rich, and polluted high-CO air over the plains. We also observed evidence of the upslope transport of the photosynthesized low-CO_2 air followed by a period of the upslope transport of high-CO_2 air resulting from reduced photosynthesis, anthropogenic pollution, and reduced turbulent mixing associated with the cloud development. Overall, the net vertical CO_2 transport by the mountain circulation throughout a day depends on the strength of the thermal forcing, the intensity of photosynthetic activity, and the magnitude of the ambient flow. Both thermal forcing and the photosynthetic activity can be strongly influenced by the diurnal variation of solar radiation and presence of clouds. Some of the ecosystem respired CO_2 can remain above the mountain ridge and remain in the lower troposphere until a strong downdraft or a strong vertical mixing event brings it down to the ground somewhere downstream.

The observations in this study imply that the net regional CO_2 ecosystem-atmosphere exchange occurs in a deep vertical and large horizontal domain and requires careful consideration of transporting and mixing processes over complex terrain. Atmospheric circulations and three-dimensional turbulent transport

of CO_2 are not limited to complex terrain. Surface heterogeneity in changes of land use and land cover, for example, can lead to spatial variations of surface heating, which could also lead to significant air circulations. Monitoring CO_2 transport by both air circulations and turbulent mixing is necessary, not only over complex terrain, but also over flat terrain.

Acknowledgment

JS would like to acknowledge the support of NCAR BGS and BEACHON programs. We would like to thank Robert Banta and Beth Holland for their helpful suggestions. NCAR is sponsored by the National Science Foundation. The University Corporation for Atmospheric Research manages the National Center for Atmospheric Research under sponsorship by the National Science Foundation. Any opinions, findings, and conclusions, or recommendations expressed in this publication are those of the authors and do not necessarily reflect the views of the National Science Foundation.

References

Ahmadov, R., Gerbig, C., Kretschmer, R., Koemer, S., Neininger, B., Dolman, A. J., & Sarrat, C. (2007). Mesoscale covariance of transport and CO_2 fluxes: Evidence from observations and simulation using the WRF-VPRM coupled atmosphere-biosphere model. *J. Geophys. Res.*, **112**, D22107, doi:10.1029/2007JD008552.

Arritt, R. W., Wilczak, J. M., &Young, G. S. (1992). Observations and numerical modeling of an elevated mixed layer. *Mon. Wea. Rev.*, **120**, 2869-2880.

Aubinet, M. (2008). Eddy covariance CO_2 flux measurements in nocturnal conditions: An analysis of the problem. *Ecol. Appl.* , **18(6)**, 1368-1378.

Banta, R.M. (1984). Daytime boundary-layer evolution over mountainous terrain. Part I: Observations of the dry circulations. *Mon. Wea. Rev.*, **112**, 340-356.

Banta, R. M. (1985). Late-morning jump in TKE in the mixed layer over a mountain basin. *J. Atmos. Soc.*, **42**, 407-411.

Banta, R. M. (1986). Daytime boundary layer evolution over mountainous terrain. Part II: Numerical studies of upslope flow duration. *Mon. Wea. Rev.*, **114**, 1112-1130.

Barr, S., & Orgill, M. M. (1989). Influence of external meteorology on nocturnal valley drainage winds. *J. Appl. Meteorl. Clim.*, **28**, 497-517.

Blumen, W. (Editor), 1990: *Atmospheric Processes Over Complex Terrain*. Meteorological Monographs, 23, No. 45. American Meteorological Society, Boston, Massachusetts, USA.

Burns, S. P., & colleagues (2011). Atmospheric stability effects on wind fields and scalar mixing within and just above a subalpine forest in sloping terrain. *Boundary-Layer Meteorol.*, **138**, 231-262. doi 10.1007/s10546-010-9560-6.

Conrad, R., & Seiler, W. (1985). Influence of temperature, moisture, and organic carbon on the flux of H_2 and CO between soil and atmosphere: Field studies in subtropical regions. *J. Geophys. Res.*, **90**, 5699-5709.

De Wekker, S. F. J., Steyn, D. G., & Nyeki, S. (2004). A comparison of aerosol-layer and convective boundary layer structure over a mountain range during STAAARTE '97. *Boundary-Layer Meteorol.*, **113**, 249-271.

De Wekker, S. F. J. (2008). Observational and numerical evidence of depressed convective boundary layer heights near a mountain case. *J. Appl. Meteorl. Clim.*, **47**, 1017-1026.

Dolman, A. J., & colleagues (2006). The CARBOEUROPE regional experiment strategy. *Bull. Amer. Meteor. Soc.*, **87**, 1367-1379.

Geiger, R., Aron, R. H., & Todhunter, P. (1995). *The Climate Near the Ground.*. Vieweg, Textbook Meteorology. pp. 528.

Gudiksen, P. H., & Shearer, D. L. (1989). The dispersion of atmospheric tracers in nocturnal drainage flows. *J. Appl. Meteorl. Clim.*, **28**, 602-608.

Kalthoff, N., Horlacher,V., Corsmeier, U., Volz-Thomas, A., Kolahgar, B., Geib, H., Möllmann-Coers, M., & Knaps, A. (2000). Influence of valley winds on transport and dispersion of airborne pollutants in the Freiburg-Schauinsland area. *J. Geophys. Res.*, **105**, No. D1, 1585-1597.

Kutsch, W., Kolle, O., Rebmann, C., Knohl A., Ziegler W., & Schulze, E. D. (2008). Advection and resulting CO_2 exchange uncertainty in a tall forest in central Germany. *Ecol. Appl.* , **18(6)**, 1391-1405.

Mahrt, L., & Larsen, S. (1990). Relation of slope winds to the ambient flow over gentle terrain. *Boundary-Layer Meteorol.*, **53**, 93-102.

McGowan, H. A. (2004). Observation of anti-winds in a deep Alpine valley, Lake Tekapo, New Zealand. *Arctic, Antarctic, and Alpine Research*, **36(4)**, 495-501.

McKendry, I. G., Steyn, D. G., Banta, R. M., Strapp, W., Anlauf, K., & Pottier, J. (1998). Daytime photochemical pollutant transport over a tributary valley lake in Southwestern British Columbia. *J. Appl. Meteorl. Clim.*, **37**, 393-404.

Orgill, M. M. (1989). Early morning ventilation of a gaseous tracer from a mountain valley. *J. Appl. Meteorl. Clim.*, **28**, 636-651.

Orgill, M. M., Kincheloe, J. D., & Sutherland, R. A. (1992). Mesoscale influences on nocturnal valley drainage winds in Western Colorado valleys. *J. Appl. Meteorl. Clim.*, **31**, 121-141.

Pérez-Landa, G., Ciais, P., Sanz, M. J., Gioli, B., Miglietta, F., Palau, J. L., Gangoiti, G., & Millan, M. M. (2007a). Mesoscale circulations over complex terrain in the Valencia coastal region, Spain — Part 1: Simulation of diurnal circulation regimes. *Atmos. Chem. Phys.*, **7**, 1835-1849.

Pérez-Landa, G., & colleagues (2007b). Mesoscale circulations over complex terrain in the Valencia coastal region, Spain—Part 2: Modeling CO_2 transport using idealized surface fluxes. *Atmos. Chem. Phys.*, **7**, 1851-1868.

Reuten, C., Steyn, D. G., Strawbridge, K. B., & Bovis, P. (2005). Observations of the relation between upslope flows and the convective boundary layer in steep terrain. *Boundary-Layer Meteorol.*, **116**, 37-61.

Rotach, M. W., & colleagues (2004). Turbulence structure and exchange processes in an Alpine valley. *Bull. Amer. Meteor. Soc.*, **85**, 1367-1385.

Rotach, M., & Zardi D. (2007). On the boundary-layer structure over highly complex terrain: Key findings from MAP. *Quart. J. Roy. Met. Soc.*, **133**, 937-948.

Seinfeld, J. H., & Pandis, S. N. (2006). *Atmospheric Chemistry and Physics: From Air Pollution to Climate Change.* A Wiley-Interscience Publication, John Wiley & Sons, Inc. pp.1232.

Sun, J., & colleagues (2007). CO_2 transport over complex terrain. *Agric. Forest. Met.*, **145**, 1-21.

Sun J., & colleagues (2010). A multi-scale and multi-disciplinary investigation of ecosystem-atmosphere CO_2 exchange over the Rocky Mountains of Colorado. *Bull. Amer. Meteor. Soc.*, **91(2)**, 209-230.

Tarr, A. M., Miller, W. L., & Zepp, R. G. (1995). Direct carbon monoxide photoproduction from plant matter. *J. Geophys. Res.*, **100**, 11,403-11,413.

Wallace, J. M., & Hobbs, P. V. (2006). *Atmospheric Science: An Introductory Survey*. Elsevier Academic Press. pp. 480.

Whiteman, C. D. (1982a). Breakup of temperature inversions in deep mountain valleys: Part I. Observations. *J. Appl. Meteorl. Clim.*, **21**, 270-289.

Whiteman, C. D. (1982b). Breakup of temperature inversions in deep mountain valleys: Part II. Thermodynamic model. *J. Appl. Meteorl. Clim.*, **21**, 290-302.

Whiteman, C. D. (1989). Morning transition tracer experiments in a deep narrow valley. *J. Appl. Meteorl. Clim.*, **28**, 626-635.

Whiteman, C. D. (2000). *Mountain Meteorology—Fundamentals and Applications*. Oxford University Press, p. 355.

Wolff, J. K., & Sherman, R. D. (2008). Climatology of upper-level turbulence over the contiguous United States. *J. Appl. Meteorl.*, **47**, 2198-2214.

Reviewed by Robert M. Banta from Earth System Research Laboratory, National Oceanic and Atmospheric Administration, Boulder, Colorado, USA; and Elisabeth Holland from Atmospheric Chemistry Division, Earth System Laboratory, National Center for Atmospheric Research, Boulder, Colorado, USA.